Field-induced delocalization and Zener breakdown in semiconductor superlattices

Field-Induced Delocalization and Zener Breakdown in Semiconductor Superlattices

B. Rosam,[1] D. Meinhold,[1] F. Löser,[1] V. G. Lyssenko,[1] S. Glutsch,[2] F. Bechstedt,[2] F. Rossi,[3] K. Köhler,[4] and K. Leo[1]

[1]*Institut für Angewandte Photophysik, Technische Universität Dresden, 01062 Dresden, Germany*
[2]*Friedrich-Schiller-Universität Jena, Institut für Festkörpertheorie und Theoretische Optik, 07743 Jena, Germany*
[3]*Instituto Nazionale per la Fisica della Materia (INFM) and Departimento di Fisica, Politecnico di Torino, 10129 Torino, Italy*
[4]*Fraunhofer-Institut für Angewandte Festkörperphysik, 79108 Freiburg, Germany*

(Received 25 June 1999)

We investigate the energy spectrum and the electron dynamics of a band in a semiconductor superlattice as a function of the electric field. Linear optical spectroscopy shows that, for high fields, the well-known localization of the Bloch states is followed by a field-induced delocalization, associated with Zener breakdown. Using time-resolved measurements, we observe Bloch oscillations in a regime where they are damped by Zener breakdown.

DOI: 10.1103/PhysRevLett.86.1307 PACS numbers: 73.21.–b, 72.20.Ht, 78.47.+p, 78.66.–w

High-field transport in solids has been investigated for many decades due to the basic interest in the physical phenomena involved and due to many important applications. Initially, the investigations were concentrated on the understanding of the electrical breakdown. A key theoretical contribution was made by Zener [1] who showed—based on Bloch's work on the motion of an electron wave packet in a solid [2]—that the onset of electrical breakdown could be related to the transition of the carriers from the valence band to higher bands (Zener tunneling).

A long-standing debate has focused on the electronic structure of a periodic potential in an electric field. In 1960, Wannier [3] discovered that the energy spectrum of a Bloch electron in an electric field F consists of equally spaced eigenvalues with energies $E_n = E_0 + neFd$, where n is an integer and d is the lattice spacing. However, he also argued that the eigenfunctions cannot be normalized and should therefore not lead to stationary states. On the other hand, the most common approximations, the discrete model [4,5], the closely related tight-binding model [6], and the one-band approximation [7,8], lead to localized wave functions, and it was a common belief for a long time that the spectrum of a Bloch electron in an electric field is discrete. This assumption was questioned by Zak [9] and, eventually, the continuous nature of the spectrum was rigorously established by Avron *et al.* [10]. Nevertheless, from the practical point of view, the notion of "Wannier-Stark resonances" is justified when the lifetime broadening is much smaller than the level spacing [11].

The invention of the semiconductor superlattice (SL) in 1970 [12] has allowed one to obtain key experimental results like the observation of negative differential velocity [13], of the Wannier-Stark ladder (WSL) with energy differences E_n in the linear optical spectra [14], and of Bloch oscillations (BO) [15], including the observation of tunable far-infrared emission [16] and the harmonic spatial motion [17]. As an alternative system, atoms in light lattices have recently been used to observe Bloch oscillations [18] and Zener tunneling [19].

During the last few years, effects based on the interaction of several bands have been explored. Resonant coupling of different Stark ladders was reported in experiment [20,21] and theory [22]. Zener breakdown in SL was explored theoretically [23], and recently, interminiband Zener tunneling was observed experimentally in the transport properties of superlattices [24]. Zener resonances in a SL with weakly coupled first miniband were observed in the intraband absorption [25]. The *dynamics* of individual carriers in SL at very high fields are experimentally unexplored. While Bloch oscillations of the carriers have been measured in the low-to-medium-field regime where the coupling of different bands is less important, data about the dynamics of carriers in the regime of Zener breakdown have not been reported.

In this Letter, we show that Zener breakdown can be observed in the *interband optical spectra* of semiconductor superlattices. We show that the field-induced Wannier-Stark localization (which is a single-band process) observed in many experiments is followed by a field-induced *delocalization* to the continuum (which is a multiband process). This delocalization is associated with Zener breakdown as observed by a decrease in oscillator strength and an increase in linewidth. By using shallow superlattices with only one electron miniband in the below-barrier region, we are able to directly address the effects of coupling of a localized state to the above-barrier continuum. Using pump-probe experiments, we explore for the first time Bloch oscillations in a regime where damping by Zener tunneling to the continuum prevails. It turns out that the Zener tunneling rate is pronouncedly different for a wave packet and a stationary state.

Shallow well heterostructures have been investigated from an application point of view for some time [26,27]. Here we use such samples to directly observe Zener breakdown due to tunneling to unbound states of above-barrier subbands [28]. We show data from two representative samples: sample A, a 76/39 Å $GaAs/Al_{0.08}Ga_{0.92}As$ SL, and sample B, a 50/54 Å $GaAs/Al_{0.11}Ga_{0.89}As$ SL. The

relevant band parameters for A/B are first electron miniband (MB) width $\Delta = 28/30$ meV, second MB width 102/130 meV, and gap between first and second MB 34/55 meV. The ratio eFd/Δ is 0.82, 1.64, and 2.46 for fields of 20, 40, and 60 kV/cm, respectively, for sample A. Values for sample B are virtually identical.

Figure 1(a) displays the experimentally observed absorption as a function of photon energy and bias field for sample A, taken at 10 K. The absorption has been differentiated with respect to the energy in order to improve the visibility of weak transitions. For fields up to 25 kV/cm, the spectra show the usual WSL both for heavy holes (hh) and light holes (lh), as observed previously [14]. For higher fields, the vertical $n = 0$ heavy-hole (hh_0) transition becomes pronounced due to field-induced localization. For fields larger than about 60 kV/cm, *the transition rapidly disappears*.

Our theoretical modeling of the linear absorption [29] is based on the stationary Schrödinger equations

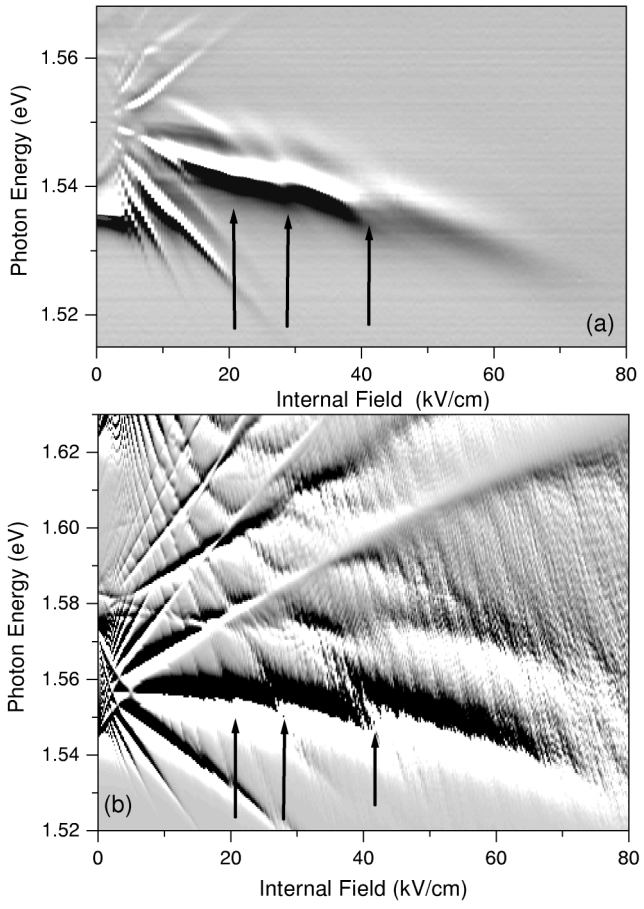

FIG. 1. (a) Gray-scale map of the differentiated absorption of shallow superlattice sample A as a function of electric field and photon energy. (b) Gray-scale map of the differentiated optical density of shallow superlattice sample A calculated using the theory described in the text. In both figures, strong anticrossings of the hh_0 transition with above-barrier transitions are labeled by arrows.

$$\left[-\frac{\hbar^2}{2m_{e,h}}\frac{d^2}{dz^2} + U_{e,h}(z) \pm eFz\right]\psi_{e,h}(z) = E\psi_{e,h}(z), \tag{1}$$

describing the individual states of electrons (e) and holes (h) within the periodic SL potentials $U_{e,h}$ subjected to a homogeneous electric field F. According to Fermi's golden rule the one-dimensional optical density of states takes the form

$$D(\omega) = \int_{-\infty}^{+\infty} dE \int_{-\infty}^{+\infty} dE' \left| \int_{-\infty}^{+\infty} dz\, \psi_{eE}(z)\psi_{hE'}(z) \right|^2 \times \pi\delta[\hbar\omega - (E + E' + E_g)]. \tag{2}$$

The free-particle absorption, which also accounts for the in-plane motion, is proportional to the integral $\int_{-\infty}^{\omega} d\omega' D(\omega')$. However, the function $D(\omega)$ is better suited for comparison with experimental absorption spectra, because the maxima of D are a good orientation for the location of the excitonic transitions (see, e.g., Fig. 4 in [30]).

Figure 1(b) shows the computed differential absorption $[dD(\omega)/d\omega]$ of sample A. For low fields, the usual WSL ladder is visible. In the field region of 20 to 40 kV/cm, several anticrossings of the hh_0 transition are visible in both theory (b) and experiment (a). These are anticrossings with the Stark ladder of the second e and hh transitions. Although this is already a transition to an above-barrier state, there are still signatures of a Wannier-Stark ladder in the optical spectrum. Because of the large bandwidth and a nearly parabolic dispersion, the associated states are delocalized.

For higher fields, the nature of the delocalization of the electron envelope wave function changes. The coupling to a continuum of above-barrier states leads to the delocalization which is clearly visible in the linear spectra: The oscillator strength of the transitions quickly disappears due to electron delocalization, in agreement with experiment. We note that the inclusion of an infinite number of bands in the theory is essential to obtain the very good agreement between experiment and theory.

Figure 2 displays three exemplary experimental absorption spectra of sample A, showing how the increase of the WSL transition strength for lower fields is followed by a decrease. The inset gives the corresponding wave functions derived from theory.

Figure 3 plots the relative oscillator strength of the hh_0 transition versus electric field. For low fields, the oscillator strength increases due to the increasing localization, as previously observed. For higher fields, there are resonances due to anticrossings, marked by arrows corresponding to those in Fig. 1. The oscillator strength then saturates and finally *decreases due to the field-induced delocalization*. It is important to note that this delocalization is not due to resonant coupling to localized states in neighboring wells, as discussed previously [20,21]. Instead, it is delocalization due to coupling to continuum states above the barriers.

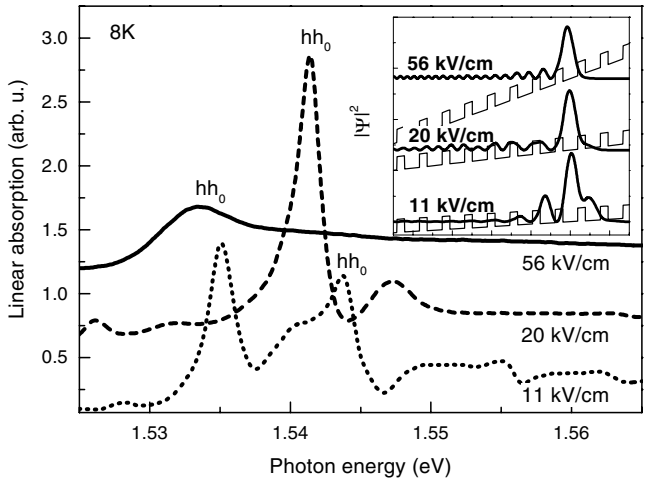

FIG. 2. (a) Absorption spectra of sample A at different fields. Inset: Calculated electron wave functions.

The analysis of the full width at half maximum of the hh_0 transition (not shown) underlines the above discussion. Initially, the linewidth is slowly increasing with field. In the high-field region, it starts to increase much more rapidly, indicating the delocalization of the wave function which is associated with a strong increase of the Zener transfer of carriers to the continuum [31].

We use two different time-resolved techniques to address the *dynamics in the Zener breakdown regime*: Pump-probe (PP) experiments [32] are used to study the *intraband* dynamics of Bloch-oscillating wave packets in sample B [33]. The inset of Fig. 4(a) shows typical traces which display the modulation due to BO. The damping of the Bloch wave packets (*intraband damping*) is determined by fitting the damping of the signal modulation. Figure 4(a) shows the intraband decay time T_{12} as a function of the field: For fields up to about 20 kV/cm, decay times depend only weakly on the field. Then, there is suddenly

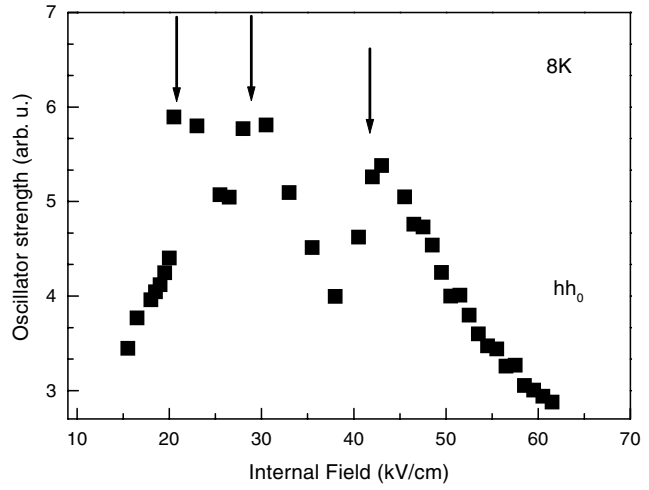

FIG. 3. Oscillator strength of sample A as a function of field. The arrows correspond to those in Fig. 1.

a threshold where the BO become very strongly damped and the decay time drops within 5 kV/cm to about 160 fs [34]. In the linear spectra, this threshold is associated with an anticrossing of the hh0 transition with a continuum resonance: Obviously, we observe here for the first time *the damping of BO due to Zener breakdown*. This effect is masked in deep SL by interface and phonon scattering [35].

We have simulated these experiments using a direct numerical solution of the semiconductor Bloch equations (SBE). In particular, in order to properly describe Zener-tunneling processes in the high-field regime, the generalized SBE formulation in [35] (i.e., including intra- as well as interminiband electric-field contributions) has been employed. The results confirm the presence of coherent Zener tunneling of electrons into the continuum, which increases with increasing field. The lower inset of Fig. 4(a) shows typical computed BO traces below (20 kV/cm) and

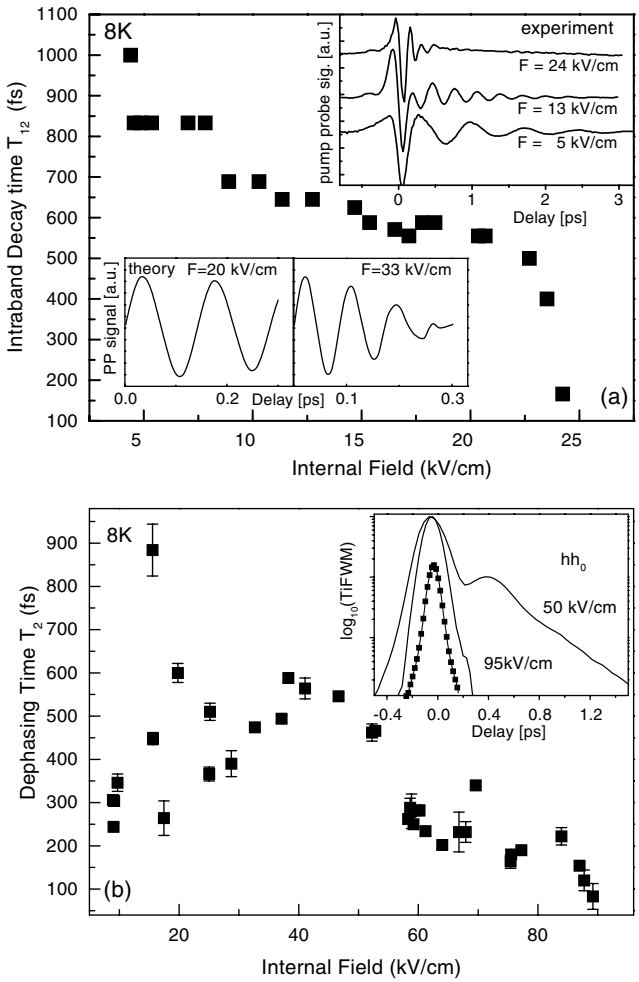

FIG. 4. (a) Intraband decay time T_{12} as a function of field for sample B. Upper inset: Typical experimental pump-probe traces; Lower inset: Theoretical intraband traces. (b) Interband dephasing time T_2 (assuming homogeneous broadening) as a function of electric field for sample B. Inset: Typical four-wave mixing traces and pulse autocorrelation.

above threshold (33 kV/cm). Below, BO are basically undamped; above, we see a very fast decay due to resonant Zener tunneling with a decay time of about 200 fs, close to the experimental value of about 160 fs. The theoretical decay times exhibit a step behavior similar to those observed in the experiment, but with a somewhat larger threshold field. This discrepancy can be ascribed to a number of phenomena not included in our theoretical modeling, e.g., intra- as well as interband Coulomb effects, band nonparabolicity, etc.

For comparison, we have also measured in sample B the *interband* coherence between the electron and hole of the hh_0 transition using transient four-wave mixing with resonant excitation of the hh_0 transition. The interband polarization decay will reflect the electron tunneling to the continuum, since the holes are much more localized. Figure 4(b) shows the field dependence of the dephasing time T_2. For higher fields, when coupling to the continuum becomes important, the dephasing time decreases continuously, in agreement with the strong increase of the line broadening. In further work, it would be interesting to study BO damping in this high-field, continuum breakdown regime. However, this is not possible for the structures studied here since the BO wave packet excitation is limited to fields of about 35 kV/cm.

We thank R. C. Iotti and M. M. Dignam for helpful discussions. We acknowledge Deutsche Forschungsgemeinschaft support (Le 747/11) and computing time from the John von Neumann Institute for Computing, Forschungszentrum Jülich.

[1] C. Zener, Proc. R. Soc. London **145**, 523 (1934).
[2] F. Bloch, Z. Phys. **52**, 555 (1928).
[3] G. H. Wannier, Phys. Rev. **117**, 432 (1960).
[4] K. Hacker and G. Obermair, Z. Phys. **234**, 1 (1970).
[5] M. Luban and J. H. Luscombe, Phys. Rev. B **35**, 9045 (1987).
[6] J. Bleuse, G. Bastard, and P. Voisin, Phys. Rev. Lett. **60**, 220 (1988).
[7] E. O. Kane, J. Phys. Chem. Solids **12**, 181 (1959).
[8] J. Callaway, *Quantum Physics of the Solid State* (Academic Press, New York and London, 1974), Pt. B, p. 465ff.
[9] J. Zak, Phys. Rev. Lett. **20**, 1477 (1968).
[10] J. E. Avron *et al.,* J. Math. Phys. (N.Y.) **18**, 918 (1977).
[11] A. Nenciu and G. Nenciu, J. Phys. A **15**, 3313 (1982).
[12] L. Esaki and R. Tsu, IBM J. Res. Dev. **61**, 61 (1970).
[13] A. Sibille *et al.,* Phys. Rev. Lett. **64**, 52 (1990).
[14] E. E. Mendez, F. Agullo-Rueda, and J. M. Hong, Phys. Rev. Lett. **60**, 2426 (1988); P. Voisin *et al.,* Phys. Rev. Lett. **61**, 1639 (1988).
[15] J. Feldmann *et al.,* Phys. Rev. B **46**, 7252 (1992); K. Leo *et al.,* Solid State Commun. **84**, 943 (1992).
[16] C. Waschke *et al.,* Phys. Rev. Lett. **70**, 3319 (1993).
[17] V. G. Lyssenko *et al.,* Phys. Rev. Lett. **79**, 301 (1997).
[18] M. Ben Dahan *et al.,* Phys. Rev. Lett. **76**, 4508 (1996).
[19] S. R. Wilkinson *et al.,* Phys. Rev. Lett. **76**, 4512 (1996).
[20] H. Schneider *et al.,* Phys. Rev. Lett. **65**, 2720 (1990).
[21] M. Nakayama *et al.,* Phys. Rev. B **44**, 5935 (1991).
[22] G. Bastard *et al.,* Phys. Rev. B **50**, 4445 (1994).
[23] J. Leo and A. MacKinnon, J. Phys. Condens. Matter **1**, 1449 (1989).
[24] A. Sibille, J. F. Palmier, and F. Laruelle, Phys. Rev. Lett. **80**, 4506 (1998).
[25] M. Helm *et al.,* Phys. Rev. Lett. **82**, 3120 (1999).
[26] K. W. Goossen, J. E. Cunningham, and W. Y. Yan, Appl. Phys. Lett. **57**, 2582 (1990).
[27] G. von Plessen, J. Feldmann, and E. O. Göbel, Appl. Phys. Lett. **63**, 2372 (1993).
[28] Deep SL are unsuitable for these investigations because resonant interminiband tunneling of below barrier minibands strongly masks the coupling to above-barrier states.
[29] S. Glutsch and F. Bechstedt, Phys. Rev. B **60**, 16 584 (2000).
[30] S. Glutsch and F. Bechstedt, Phys. Rev. B **57**, 11 887 (1998).
[31] Since we study the wave function delocalization in a superlattice, we cannot observe the catastrophic electrical Zener breakdown seen in a bulk sample: there, the transfer of a large number of carriers from the filled valence band leads to an increase of the number of mobile carriers by many orders of magnitude, whereas in a SL, only the comparatively small number of photoexcited carriers is transferred to higher minibands. In the current-voltage curves of our sample, we thus cannot observe a significant effect.
[32] Conditions for the PP and FWM experiments are as follows: Excitation density on the order of 10^9 cm^{-2}; for PP excitation, the hh_0 and hh_{-1} transitions are excited with 80 fs pulses; and for FWM excitation, the pulse duration is varied (100–300 fs) to selectively excite the hh_0 transition.
[33] Linear spectra of sample B are almost identical to sample A; the main difference being a weaker coupling to the continuum in sample B due to somewhat higher barriers.
[34] Because of the progressing WSL localization an excitation of a Bloch oscillating wave packet is not possible for higher fields.
[35] F. Rossi, topical review on *Coherent phenomena in semiconductors,* Semicond. Sci. Technol. **13**, 147 (1998); F. Rossi, in *Theory of Transport Properties of Semiconductor Nanostructures,* edited by E. Schöll (Chapman & Hall, London, 1998), p. 283.